IEEE Access
Multidisciplinary | Rapid Review | Open Access Journal

Received May 4, 2022, accepted May 20, 2022, date of publication June 2, 2022, date of current version June 7, 2022.

Digital Object Identifier 10.1109/ACCESS.2022.3179716

Comparison of Different Power Balance Control Methods for Battery Energy Storage Systems on Hybrid Marine Vessels

JAN-HENRI MONTONEN, TUOMO LINDH, ANDREY LANA, PASI PELTONIEMI, (Member, IEEE), ANTTI PINOMAA, KYÖSTI TIKKANEN, AND OLLI PYRHÖNEN, (Member, IEEE)

LUT School of Energy Systems, Lappeenranta–Lahti University of Technology (LUT), 53850 Lappeenranta, Finland

Corresponding author: Jan-Henri Montonen (henri.montonen@lut.fi)

This work was supported by the Business Finland through the Integrated Energy Solutions to Smart and Green Shipping (INTENS) Research.

ABSTRACT In this paper, different power balance control methods for hybrid marine vessels are analyzed. First, the power grid of a marine vessel is modeled using MATLAB and Simulink. Simulations are then performed using real power plant load data captured from an actual vessel. Isochronous control is used to control the power of the diesel gensets, and different control methods, such as isochronous control and average load power estimation, are used for the battery energy storage system. The system is simulated with different control parameters, and the effects of parameter changes are presented. It is shown that these presented control schemes can be adapted to manage the energy balance in a hybrid vessel, thereby enabling efficient use of the battery energy storage system. A diesel genset and battery energy storage system failure during a dynamic positioning operation is also simulated, and the effect of the failure on the frequency of the power grid of the vessel is presented.

INDEX TERMS AC grid, battery energy storage system, dynamic positioning, hybrid vessel, isochronous control, simulation, Simulink.

I. INTRODUCTION

Battery energy storage systems (BESS) can be used in marine vessels to attain improved fuel economy and to achieve reduced emissions [1]. One application of a BESS is peak power shaving, in which power peaks are shaved by drawing power from the BESS, thus enabling steady load on the power plant diesel engines [2], [3]. Hence, for the performance in maritime operations, the rated power of the diesel engines can be smaller than in a similar vessel not equipped with a BESS. In this manner, hybridization can bring benefits in terms of the lower CAPEX and OPEX of a marine vessel [4]. In this work, an Offshore Supply Vessel (OSV) is used as a case vessel. OSVs are a vessel type used for supplying cargo and personnel to oil drilling or other offshore construction sites. In addition, OSVs can also be equipped to operate as anchor handling, sea exploration, or accommodation vessels. When on duty, OSVs can use their thrusters and main propulsion to stay in position relative to the sea bed or a moving object. This is called dynamic positioning (DP) [13]. The average power demand in the DP mode is small compared with the power demand in the cruise mode. However, load transients can be fast, especially in rough sea conditions. In many cases, the need to accommodate load transients is handled by running more gensets than what would be required by the average load power demand.

The BESS needs to be controlled in an appropriate way to achieve a high fuel efficiency of the gensets and to ensure a stable network frequency during load transients and a stable vessel operation during fault situations. Different methods for vessel power balance control for vessels with and without a BESS have been presented in the literature to mitigate the fluctuating load power demand caused by the propulsion. Model-based predictive control for battery power has been presented in [5], [6], and different types of energy storages have been suggested in the literature. For example, the use of flywheels, batteries, and ultracapacitors has been studied for the mitigation of power fluctuation

The associate editor coordinating the review of this manuscript and approving it for publication was Youngjin Kim.

This work is licensed under a Creative Commons Attribution 4.0 License. For more information, see https://creativecommons.org/licenses/by/4.0/

in vessel power distribution systems in [7]–[10]. In [11] a power management method based on filtering load power is presented as means for load sharing between power sources with different response times. In [10], fuzzy logic control was used to calculate a power reference for a hybrid energy storage consisting of a battery and an ultracapacitor. Thruster power was modulated to mitigate the load variations caused by other power consumers on the vessel in [12]. During dynamic positioning (DP), however, this approach causes small deviations to the commands given by the DP system, which may be undesirable in some cases. Additionally, thrusters can be driven in opposite directions to enable fast switching of thrust direction by reducing thrust from the opposite direction [14], [16]. Running thrusters in opposite directions, however, reduces the energy efficiency of the vessel. Thrusters can also be used to mitigate power fluctuations when there is a sudden drop of load power by increasing the thruster power [12]. Also, strategic loading of the energy storage to improve fuel efficiency has been studied in [15]. It was shown in [17] that by equipping an OSV with a BESS, transients can be taken from the BESS and the average power can be produced by running fewer gensets. These gensets then run on a higher load and use less fuel per produced kWh.

This study investigates isochronous-control-based power control methods for a BESS in hybrid vessels using a detailed simulation model. The model allows to investigate power, frequency, voltage, and current from the grid, instead of only power flow. Data recorded from an actual vessel is used as load power data. Three methods are proposed to run a BESS in a marine vessel already equipped with isochronous load sharing for the gensets. This enables the retrofitting of a BESS to a vessel already using isochronous control for the gensets and a constant-frequency AC grid for power distribution. To the best of the authors' knowledge, isochronous control has not been introduced as a control method enabling this advantageous usage of a BESS. It is interesting to compare the traditional isochronous control with the average power control in order to reveal the performance of both control laws in hybrid vessels.

II. CONTROL METHODS

Isochronous control is used to control the gensets and to enable load sharing in a powerplant. The study considers three control methods. In the first control scheme, the BESS is treated like a genset. The power reference for the BESS is formed using the isochronous control scheme described in Section II-A.

The second control method calculates an average load power estimate and uses the difference between the estimated and actual load power as the power reference for the BESS. This control scheme is presented in Section II-B. The third control scheme is start–stop, which is based on an isochronous control in which one diesel genset (DG) is running constantly and one is started and stopped based on the load power demand. This approach increases fuel efficiency as the DGs run on a higher load. The control scheme is presented in Section II-C.

TABLE 1. Example of the diesel genset power division for a four-genset isochronous system.

Genset number	p_i	b_i	$p_{\text{ref, i}}$
1	0.8	0	0.6
2	0.5	0.2	0.8
3	0.8	0	0.6
4	0.5	0	0.6

A. ISOCHRONOUS CONTROL

In the isochronous load sharing mode, each genset compares its produced power against the biased and weighted average produced power per genset as presented in (1). The effect of biasing and weighting is then removed from the power references of the gensets, (2). The biased average power $\overline{p}$ is calculated as

$$\overline{p} = \frac{1}{n}\sum_{i=1}^{n}\frac{p_i - b_i}{c_i} \tag{1}$$

where p_i is the produced power of the genset i, c_i is the load gain, b_i is the load bias, and n is the number of running gensets. With the load gain and the load bias, a genset can be ''fooled'' to produce more power as it believes that the other gensets are producing more power than it is. The load bias can be used to set a constant difference between the produced powers of the gensets. The load gain can be used to set a constant ratio between the produced powers of the gensets. The load gain and the load bias are useful when unbalanced load sharing is desired, e.g., to save fuel or to reduce the load on one genset. The power reference for the genset i is calculated as

$$p_{ref,i} = \overline{p}c_i + b_i \tag{2}$$

For clarification, an illustrative example of a four genset system is given in Table 1. For simplification, c_i is assumed to be equal to one. The actual genset power in per units is shown in the p_i column, and the load bias is shown in the b_i column. The nominal power of the genset corresponds to 1 p.u. The average power $\overline{p}$ is calculated using (1) and the values in the p_i and b_i columns. The average power of $\overline{p} = 0.6$ p.u. is attained.

The power reference for each genset is calculated using (2), and it is shown in the P_{ref} column. A load bias of 0.2 p.u. was set for DG2, which can be seen as a 0.2 p.u. higher power reference compared with the other gensets. The load gain c_i was set to 1 for simplification.

The engine power is controlled using a PID fuel rate controller. The controller error signal is a combination of power and speed errors

$$e = K_1(p_{\text{ref}} - p_{\text{act}}) + K_2(\omega_{\text{ref}} - \omega_{\text{act}}) \tag{3}$$

where K_1 and K_2 are the gains that are used to weight the power reference or the frequency reference. ω_{ref} is constant 1.0 p.u. [18].

Isochronous control is also used to control the power reference going to the BESS. The power reference is formed by:

$$p_{\text{ref,BESS}} = K_1(\overline{p}c_{\text{BESS}} + b_{\text{BESS}}) + K_2(K_p e(t) + K_i \int_0^t e(\tau)d\tau) \quad (4)$$

where $e(t) = \omega_{\text{ref}} - \omega_{\text{act}}$. Equation (4) does not take the State-of-Charge (SOC) of the BESS into account. In a real-world case, SOC control would be mandatory, because otherwise the control scheme would drain the battery. The SOC control could be implemented as it was done in the start–stop case in Section II-C by adding an additional P-type controller to $p_{\text{ref,BESS}}$. Then, (4) would be:

$$p_{\text{ref,BESS}} = K_1(\overline{p}c_{\text{BESS}} + b_{\text{BESS}}) + K_2(K_p e(t) + K_i \int_0^t e(\tau)d\tau) - K_{\text{p,SOC}}(SOC_{\text{ref}} - SOC_{\text{act}}) \quad (5)$$

where $K_{\text{p,SOC}}$ is the gain of the SOC controller, SOC_{ref} is the SOC reference value, and SOC_{act} is the actual value of the BESS SOC. The SOC controller is used to produce an offset to the $p_{\text{ref,BESS}}$, which causes the BESS to charge or discharge over time. The integral part is omitted from the controller, because the purpose of this SOC control is not to drive the SOC to its reference value. The purpose of the SOC controller is to prevent overcharging and overdischarging and to make sure that there is energy in the battery for the frequency control. A PI-type controller could also be used, but the integration time would have to be long in order to prevent power fluctuation of the DGs caused by the SOC control.

B. AVERAGE LOAD POWER ESTIMATION

The power reference for the BESS is calculated using the difference between the current load power and the average load power:

$$P_{\text{ref,batt}} = P_{\text{load}} - P_{\text{ave}} \quad (6)$$

where P_{load} is the actual consumed power, and P_{ave} is the calculated average power over the calculation period. P_{ave} is calculated by using a moving average filter of

$$p_{\text{ave}}(n) = \frac{1}{M}[p_{\text{load}}(n - M - 1) + \ldots + p_{\text{load}}(n)] \quad (7)$$

where M is the length of the moving average window. Average power can be calculated during operation, and M and the sample time should be selected so that enough averaging is obtained but the delay caused by the filter is not too long. The selection of the filter length requires adaptation, manual or automatic. A simple moving average can be replaced by a predictive estimator [5], [19].

C. START–STOP

The start–stop enables the shutdown of superfluous gensets when the load power demand is low enough and the reduced number of gensets are capable of producing the average load. Load transients can be handled by the BESS. In this mode, one genset runs constantly and one genset is started and stopped according to the load demand. All gensets are controlled using the isochronous control described in Section II-A. The control weight parameters K_1 and K_2 are changed based on the number of running gensets. During the simulation, one genset runs constantly. When only one genset is running, it is on the 100% frequency control. When the second genset is started, the first genset remains mainly in the frequency control mode, and the second one is mainly in the power control mode. The start and stop of the second genset are determined by the load power limits. If the load power is higher than the start limit, the genset is started. When the load power goes below the stop limit, the genset is stopped.

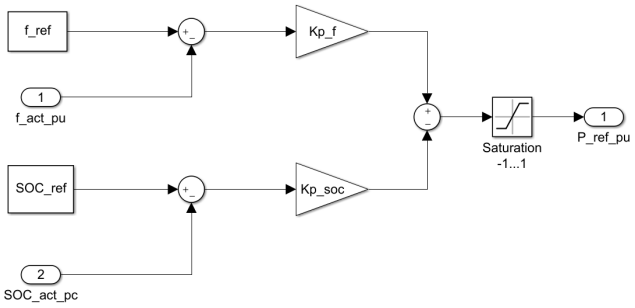

FIGURE 1. Power control scheme of a battery energy storage system (BESS) in the start–stop simulation.

The power reference for the BESS is formed as a sum of two P-type controller outputs. The first is for the AC network frequency control and the second for the SOC control of the battery. The BESS power and SOC control is illustrated in Fig. 1. In this case, the BESS power control is a modified isochronous control with weights $K_1 = 0$ and $K_2 = 1$ with the SOC control by the added P-type controller parallel to the frequency control. The integral part was removed from the frequency controller, because the BESS is supposed to participate in peak load shaving only, i.e., it should not take part in the frequency control in the steady state.

III. SIMULATION MODELS

MATLAB/Simulink is used for the simulation of the vessel power system and the proposed control. The simulation models are built from the main components such as the generator set, the BESS, the propulsion load, and the hotel load. These main components are described in the following subsections. The components are built from fundamental blocks and Simscape blocks. The simulation models are continuous time models, but a discrete solver with a 50 μs timestep is used for the Simscape models.

The vessel model is built based on Single Line Diagram (SLD) and component data of the actual vessel. A simplified SLD of the case vessel is shown in Fig. 2, and the Simulink model is presented in Fig. 3.

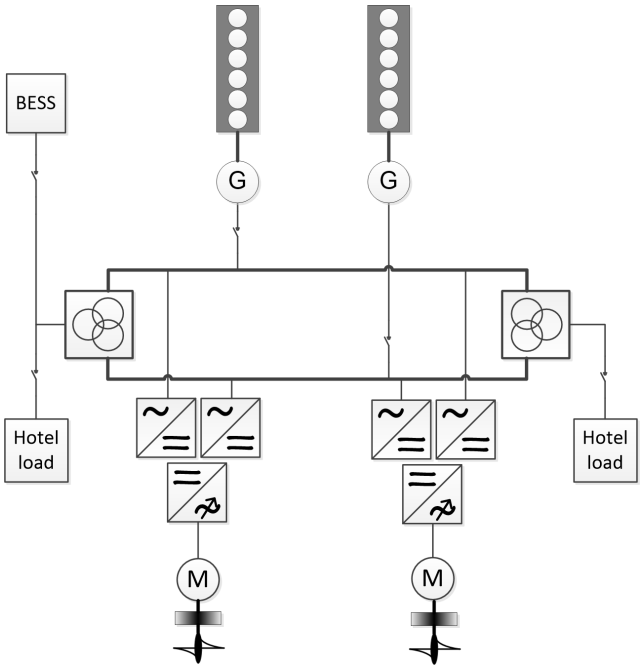

FIGURE 2. Offshore supply vessel (OSV) single line diagram (SLD) from which the Simulink model is built.

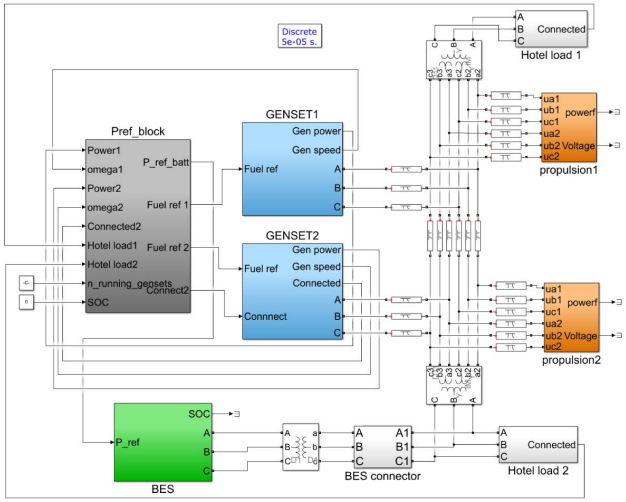

FIGURE 3. Top level of a hybrid OSV simulation model. The model contains diesel gensets (blue blocks), the BESS (green block), propulsion loads (orange blocks), the power control (grey block), and the hotel load (white blocks near the propulsion loads).

A. DIESEL GENSET

The diesel genset model is a transfer function model tuned to have a similar response to the real diesel genset in the vessel. A model presented in [3] could also be used, but it would require many engine-specific parameters, which can be hard to acquire. The diesel genset model is the model used previously in the simulations presented in [17]. The model consists of a diesel engine model and a generator model. Fig. 4 describes the top level of the diesel genset model. The generator model in Fig. 4 is a standard Simscape library synchronous motor block.

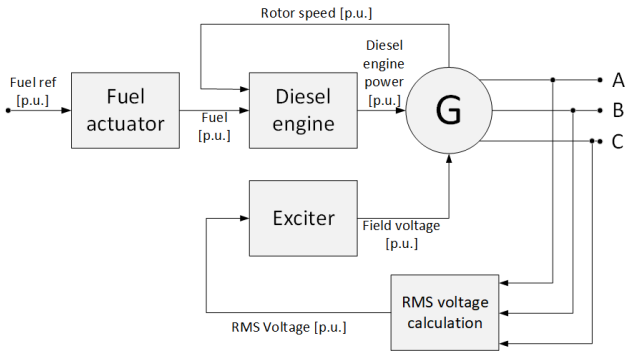

FIGURE 4. Diesel genset model consisting of a diesel engine model and a generator model.

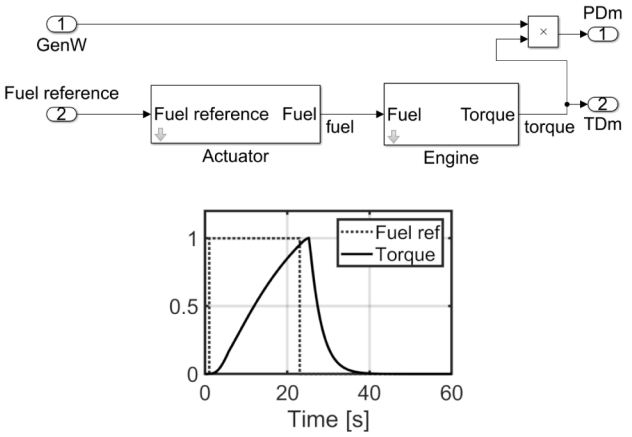

FIGURE 5. Diesel engine model block diagram and a step response of the Actuator–Engine system from the fuel reference to the torque of the diesel engine.

The diesel engine model consists of the fuel actuator and the engine itself, as shown in Fig. 5. The input to this block (fuel reference) comes from an external power control block, which is simulation case-specific. The diesel engine model block outputs power and torque.

The actuator model in Fig. 5 is shown in detail in Fig. 6. The engine model is presented in Fig. 7. The produced torque of a diesel engine is a product of air and fuel. A three-second delay model for the increase of fuel injection is used. The turbo delay constitutes the longest delay in the system. The delay is modeled with a first-order transfer function in which the time constant can be tuned to produce the fastest possible gas circulation dynamics or the dynamics that follow the soot production restrictions given to the diesel by the manufacturer [20].

B. BATTERY ENERGY STORAGE SYSTEM

The top level of the battery energy storage system is presented in Fig. 8. The BESS model contains a battery model and a grid converter model. The battery model is a standard Simscape battery model, which can be parameterized to fit each simulation case.

The grid converter is controlled by a power reference signal coming from an external power reference block. The power

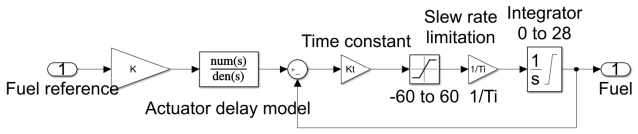

FIGURE 6. Actuator model of the diesel engine.

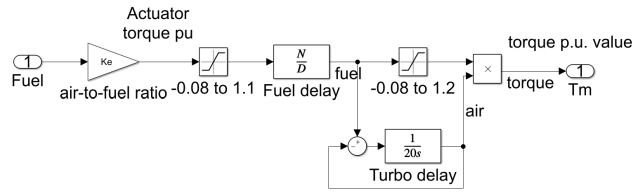

FIGURE 7. Contents of the engine model.

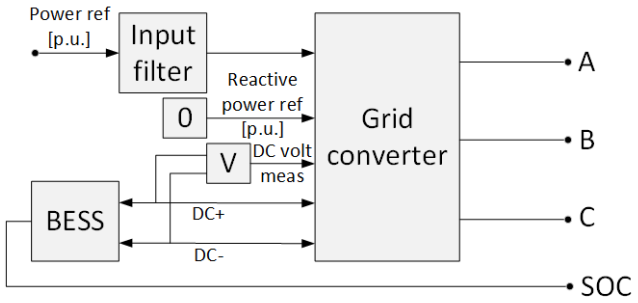

FIGURE 8. Top level of the BESS model. The model consists of a Simscape battery model and an averaging grid converter model.

reference is fed to the current controller of the grid converter as the i_d current reference. The grid converter keeps track of the grid angle by a phase-locked loop. The converter model is simplified to reduce the computational load and does not contain switches; they are replaced with voltage sources. This type of model is called an averaging model. The model is based on the model presented in [21] and [22] with the phase-locked loop presented in [23].

C. PROPULSION LOAD

The propulsion load block models the whole propulsion load of the vessel, i.e., the main propulsion and the thruster loads. The model does not contain a model of an actual drive; rather, the propulsion drive is modeled by a controlled current source that sinks power from the DC link. The model consists of a power transformer model, two diode bridge models, a DC link model, and a current source model (see Fig. 9). The propulsion power data (from an actual vessel or artificially generated test data) can be loaded from a text file. The DC link model of Fig. 9 is presented in Fig. 10.

D. HOTEL LOAD

The hotel load comprises all loads other than the propulsion load. The hotel load consists mainly of lighting, pumps, fans, and other electrical systems on the vessel. The hotel load is

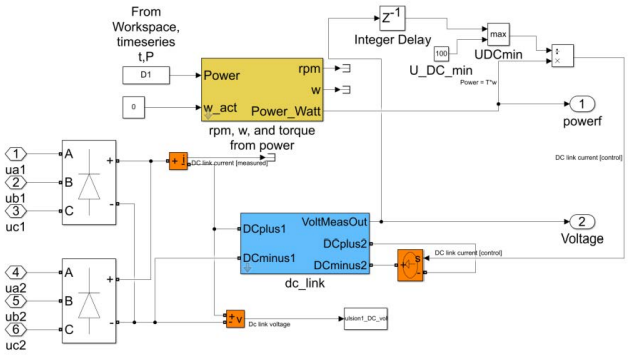

FIGURE 9. Top level of the propulsion model. The model consists of two diode bridge models, a DC link model, and a current source model.

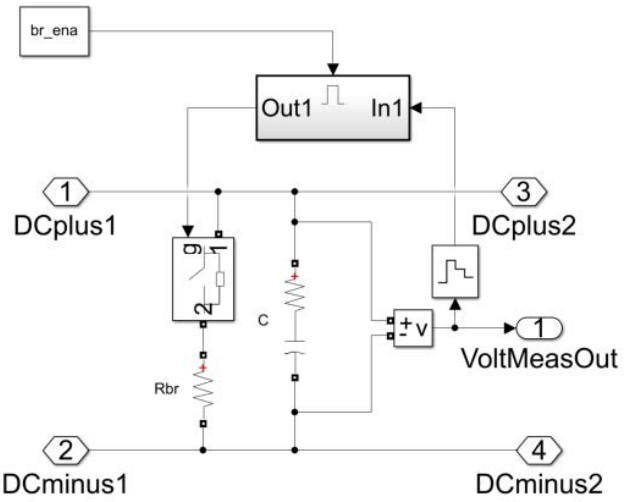

FIGURE 10. DC link model of a propulsion load model.

modeled using a Three-Phase Parallel RLC Load model from the Simscape library, as illustrated in Fig. 11. The hotel load power remains static during the simulation. The total hotel load value used in the simulations is 400 kW. The three-phase Breaker and Hotel load connector blocks connect the load to the Power Distribution System (PDS) after 60 s from the simulation start. The delay is to prevent a load impact on the gensets while they are spooling up. The three-phase load and breaker models are connected with PI section cable models.

IV. RESULTS

The simulation model was run using the load power data presented in Fig. 12. The load power consists of the static base load (hotel load) and the dynamic thruster and propulsion load. The data were obtained from an actual vessel, and they depict loading during the DP mode. These load power data are used in all the simulated cases, except for the start–stop case where higher power consumption is needed and artificial test data are used. The simulations tested various scenarios, such as:

- Loading in DP-mode
  - Traditional isochronous control without a BESS

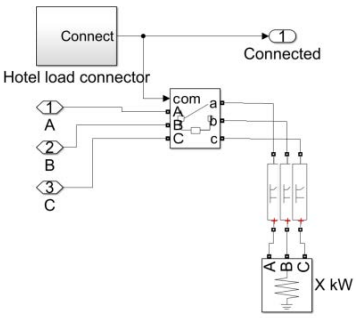

FIGURE 11. Hotel load model consisting of a three-phase breaker model and a three-phase parallel RLC load model.

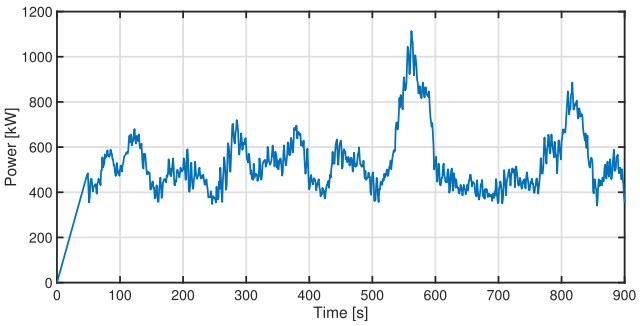

FIGURE 12. Load power used in the simulations.

  - Modified isochronous control with a BESS
    - BESS power reference from the isochronous control
    - BESS power reference from the average load power estimation
    - Start–stop with a BESS
- Robustness during malfunction
  - Genset failure
  - BESS failure

The parameters of the different simulation model components are presented in Table 2. These parameters are kept constant during simulations. The table includes references to the figures and equations where the component is displayed.

A. ISOCHRONOUS CONTROL WITHOUT A BESS

The OSV model is simulated without a BESS in four different isochronous cases to test the effect of different load sharing parameters. Case 4 tests whether the vessel is able to run in the DP mode using only one genset because of the small load power. The studied cases are:

- Two gensets running, equal load sharing (Case 1)
- Two gensets running, load gain set (Case 2)
- Two gensets running, load bias set (Case 3)
- One genset running on speed reference (Case 4)

The parameters of these cases are presented in Table 3.

Fig. 13 and Fig. 14 present the network frequency and the genset power during the simulations. Fig. 13 shows that one genset alone is unable to keep the network frequency near the setpoint. Although one genset is able to produce sufficient power for the DP operation, the dynamic response of one genset is not fast enough and the network frequency never quite reaches the setpoint. Two gensets have sufficiently fast dynamics to be able to produce the required thruster power transients. Fig. 13 also shows that varying the isochronous control parameters (load gain and load bias) under load variations does not have a significant effect on the variation in frequency. Genset power while using different isochronous parameters is presented in Fig. 14. The figure shows how the different isochronous parameters change the load sharing between the gensets. Equal load sharing parameters result in equal load sharing among the gensets. Setting the load bias or the gain will result in one genset producing the set amount of more power than the other.

When using equal load sharing (Case 1), both gensets produce the same power ($c = 1$ and $b = 1$). In Case 2, $c = 1.5$ for DG1 and $c = 0.5$ for DG2. Consequently, DG1 will produce 1.5 times the average power, and DG2 will produce 0.5 times the average power. In Case 3, the load bias is set so that DG1 will constantly produce 20% over the

TABLE 2. General model parameters that remain constant during simulations.

Unit	Parameter	Value
BESS	Nominal power	3.1 MW
	Capacity	310 kWh
	Nominal DC voltage	1050 V
	C-rate	10
BESS isochronous control (Eq.4)	K_1	0.7
	K_2	0.3
	b_{BESS}	0
	c_{BESS}	1
	K_p	10
	K_i	0.01
BESS start–stop (Fig. 1)	$K_{\text{p,f}}$	10
	$K_{\text{p,soc}}$	0.01
Diesel genset: actuator (Fig. 6)	K	1.4286
	Actuator delay model	$\frac{1}{0.025s+1}$
	Gain K_t	8.33
	Integration time T_i	1
Diesel genset: engine (Fig. 7)	Gain K_e	1
	Fuel delay model	$\frac{1}{3s+1}$

TABLE 3. Simulation parameters of different isochronous cases without a BESS.

Genset nbr	Parameter	Case 1	Case 2	Case 3	Case 4
1	K_1	0.3	0.3	0.3	0
	K_2	0.7	0.7	0.7	1
	c	1.0	1.5	1.0	1.0
	b	0	0	0.2	0
2	K_1	0.7	0.7	0.7	n/a
	K_2	0.3	0.3	0.3	n/a
	c	1.0	0.5	1.0	n/a
	b	0	0	0	n/a

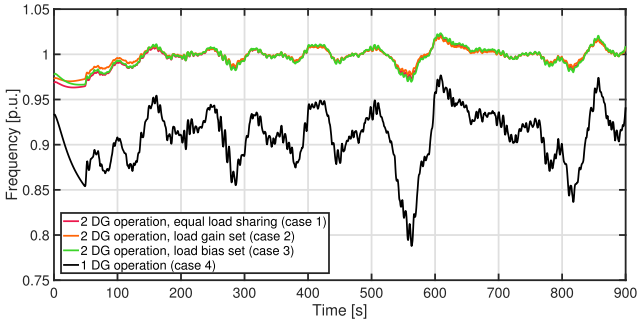

FIGURE 13. Generator speed (also AC-grid frequency) in different isochronous modes.

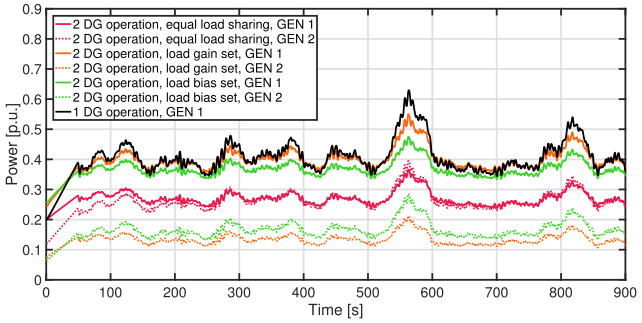

FIGURE 14. Generator power in different isochronous modes.

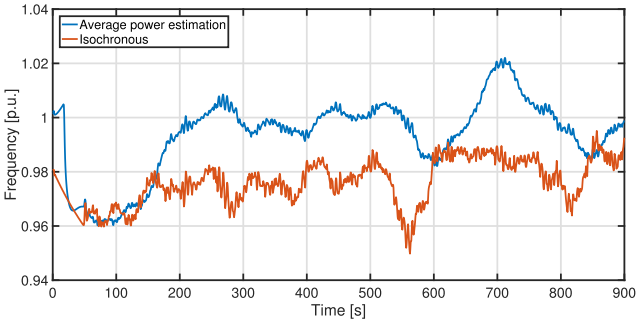

FIGURE 15. Frequency of the AC grid in one diesel genset operation with the BESS.

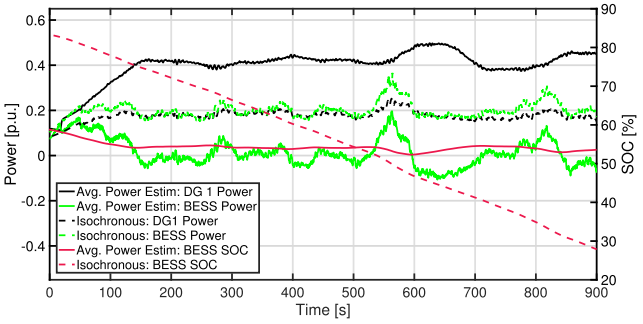

FIGURE 16. Diesel genset and BESS power while in the DP mode and running only one genset.

average power. In Case 4, only one genset is running. In this case, it runs only on the frequency reference ($K_1 = 0$ and $K_2 = 1$).

The mean value and variance of the AC network frequency are presented in Table 6 for all the simulated cases. It can be seen from the table that the isochronous load sharing parameters (b, c) have a very small effect on the frequency of the AC network.

B. ISOCHRONOUS CONTROL WITH A BESS

The behavior of the BESS when included in the isochronous control is analyzed in the following simulation. A BESS model was added to the simulation model, and the system was simulated using the load power data in Fig. 12. In the simulation, only one genset is running and the BESS supports this genset. Average load power estimation and isochronous control are used to control the power of the BESS.

When using isochronous control, the BESS is treated like a genset. The genset runs primarily on frequency reference ($K_1 = 0.3$ and $K_2 = 0.7$), and the BESS runs primarily on power reference ($K_1 = 0.7$ and $K_2 = 0.3$). Both have equal load sharing parameters ($c = 1$ and $b = 0$). The power reference for the BESS is formed by (4).

When using the power reference for the BESS from the average load power estimation, the power reference is formed as described in Section II-B as the difference between current power consumption and filtered power consumption. The length of the averaging filter used is 120 s.

From Fig. 15, it can be seen that running the BESS with a power reference from the average load power estimator gave closer to the 1 p.u. frequency during the simulation than the alternative method where the BESS is treated like a genset. Table 6 shows that the mean frequency value difference is 1.7%. The difference in variance is small between the two methods. According to Table 6, the isochronous control results in a smaller variance in the AC frequency than the average load power estimation. However, if we neglect the droop at the beginning of the simulation, the average load power estimation results in a smaller variance.

The sudden load increase at t=550 s causes a smaller drop in the AC frequency when using the average load power estimation than with the isochronous control. When using the average load power estimation, the BESS power reference increases immediately when the load power increases, but when using the isochronous control for the BESS, the frequency must first drop so that a frequency error to which the controller can react will form.

Fig. 16 presents the genset and BESS power during the simulated DP operation. When running the BESS with the average load power estimation, the BESS operates in the peak-shaving mode, whereas the genset produces the base load. The average BESS power is close to zero, and thus, the BESS is charged and discharged during the operation and the SOC does not drift. The power reference sent to the BESS from the average load power estimation is not shown in the figure, because it would be below the actual power curve of the BESS.

When running the DG and the BESS on isochronous load sharing, both produce the same power and the BESS is

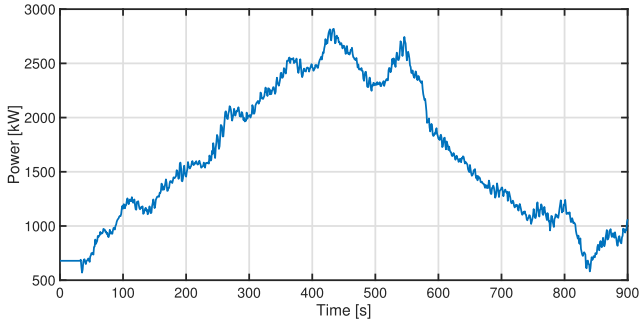

FIGURE 17. Artificial load signal used in the start–stop simulations.

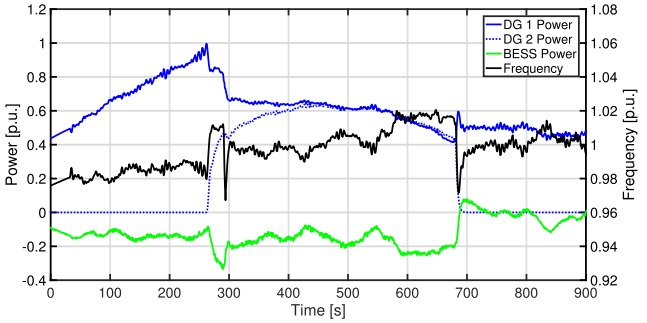

FIGURE 18. AC network frequency, genset power, and BESS power during the start–stop simulation.

TABLE 4. Genset parameters of the start–stop simulation.

Genset nbr	Parameter	1 DG Operation	2 DG operation
1	K_1	0	0.3
	K_2	1	0.7
	c	1	1
	b	0	0
2	K_1	n/a	0.7
	K_2	n/a	0.3
	c	n/a	1
	b	n/a	0
	start limit	n/a	2000 kW
	stop limit	n/a	1500 kW

discharged during the operation. A BESS charge controller was not used in this simulation, but the controller described in Fig. 1 could be used to modify the power reference as the SOC drops. Alternatively, when the lower limit of the BESS SOC is reached, charging of the battery is started and another genset must possibly be started.

C. START–STOP

The load power signal is artificial in this simulated case. An artificial load signal was used to achieve high enough power consumption to justify the starting of another genset. The load signal is created by adding a triangular wave to the DP load signal described in Fig. 12. The triangular wave has a peak-to-peak amplitude of 2000 kW, an offset of 1000 kW, and a ramp of 5kW/s.

In the simulation, genset 1 (DG1) is running constantly and genset 2 (DG2) is started and stopped according to the load power demand. The start and stop limits are given in Table 4. When running on one genset, DG1, it is on the 100% frequency control ($K_1 = 0$, $K_2 = 1$). When DG2 is started, DG1 changes to 70% frequency control and 30% power control ($K_1 = 0.3$ and $K_2 = 0.7$). DG2 runs mainly in the power control mode ($K_1 = 0.7$), but it also participates in the frequency control by 30% ($K_2 = 0.3$). The genset parameters used in the simulation are given in Table 4.

Fig. 18 presents the AC network frequency, genset powers, and the BESS power during the start–stop simulation. The start and stop of genset 2 are visible in the network frequency.

TABLE 5. Genset parameters before and after the BESS failure.

Unit	Parameter	Before fault	After fault
DG1	K_1	0	0.3
	K_2	1	0.7
DG2	K_1	n/a	0.7
	K_2	n/a	0.3

However, the change in frequency is less than 5%, and the frequency stays between 95% and 105% of the nominal frequency that the ship's PDS should be able to tolerate [24]. The frequency drops could be mitigated by ramping the power from one genset to another before shutting off the genset. In an actual vessel, these smooth start–stop functions would have to be in the power management system (PMS). Building the complete PMS into this simulation was beyond the scope of this paper.

D. FAULT CASES

Stability of an islanded grid is often studied by dropping generators off the grid or by introducing load spikes to the grid [26]. Malfunction of the BESS inverter and a genset fault during DP operation were simulated to study the stability of the grid. The DP load power data given in Fig. 12 were used in both fault case simulations.

First, a BESS failure was simulated. In the simulation, the OSV is in the DP mode and running one genset and the BESS. The genset is 100% in the frequency control mode. The power reference for the BESS is formed using two P-controllers: one for the frequency and one for the SOC of the battery, as shown in Fig. 1. A BESS failure occurs at $t = 200\ s$. The BESS is disconnected from the PDS and Genset 2 is started. During the fault, isochronous control parameters change as shown in Table 5.

The AC network frequency, genset powers, and the BESS power in the BESS malfunction simulation are presented in Fig. 19. The figure shows that the AC network frequency fluctuates less when the BESS is in operation. The BESS and Genset 1 share the load, but as the SOC of the BESS decreases slowly, the power reference for the BESS falls slowly. The fault occurs at $t = 200s$, Genset 2 starts to produce power

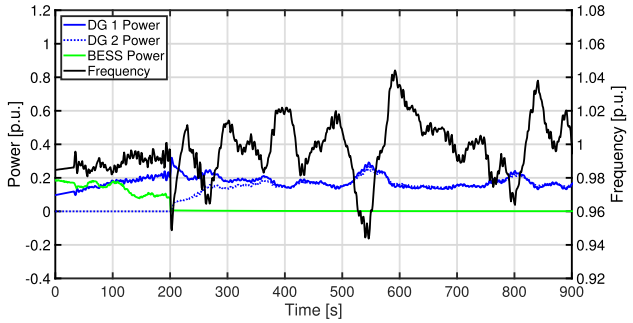

FIGURE 19. Genset and BESS power and AC network frequency during the BESS fault simulation. The fault occurs at $t = 200$ s.

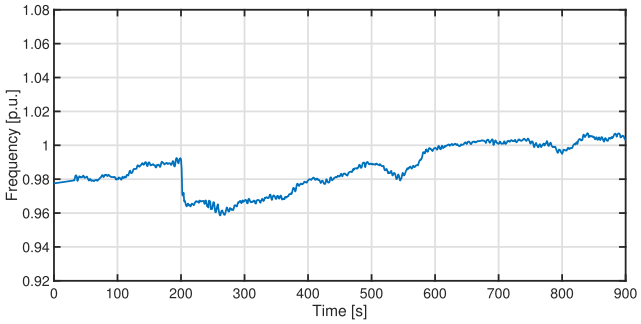

FIGURE 20. AC network frequency during genset failure simulation. The fault occurs at $t = 200$ s.

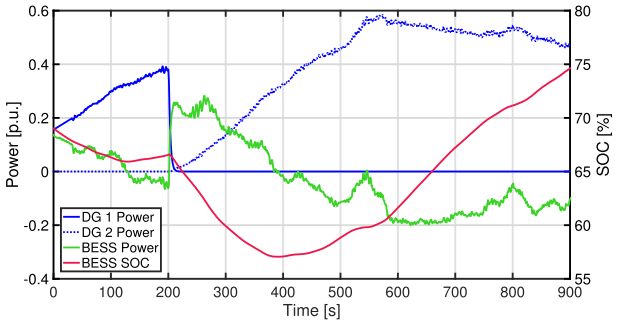

FIGURE 21. Genset and BESS power and BESS SOC during the genset failure simulation. The fault occurs at $t = 200$ s.

immediately. In this simulation, it was assumed that Genset 2 is already running synchronized to the grid with a zero power reference in order to be able to start producing power quickly, if required, for example in critical DP operations. Gensets 1 and 2 go to isochronous load sharing according to Table 5. When a BESS fault occurs, the dynamic response of the one running genset is insufficient to respond to the load power changes caused by the DP operation, and therefore, a second genset must be started, even though the rated power of one genset should be sufficient to produce the power required for the DP operation. The AC frequency drops to around 0.95 p.u. when the BESS fault occurs. Despite the fault, the load power remains as the DP operation load power depicted in Fig. 12. Load shedding could be done in a fault situation on an actual vessel to reduce the load on the remaining gensets and the risk of a blackout [25].

TABLE 6. Mean and variance of the AC network frequency in different simulations.

Figure	Case	Mean	Variance
13	Isoch. w/o BESS case 1	0.9962	1.3971e-4
13	Isoch. w/o BESS case 2	0.9975	0.9557e-4
13	Isoch. w/o BESS case 3	0.9968	1.3607e-4
13	Isoch. w/o BESS case 4	0.9083	9,6966e-4
15	With BESS avg. pwr. estim.	0.9936	1.9714e-4
15	With BESS isochronous	0.9763	0.6692e-4
18	Start-stop	0.9970	1.2608e-4

The second fault case simulates a genset fault during DP operation. The OSV is performing the DP operation using DG1 and the BESS. At $t = 200s$, DG1 develops a fault and shuts down. DG2 starts immediately and continues operation in the 100% frequency control mode ($K_1 = 0$ and $K_2 = 1$). The BESS provides the required power during the genset switch. This simulation, too, assumes that DG2 is already synchronized to the network and running on a zero power reference in order to start producing power quickly, if required.

The AC network frequency during the malfunction simulation is presented in Fig. 20 and the genset and BESS power in Fig. 21. Figs. 20 and 21 show that the genset fault causes a less than 0.03 p.u. drop in the frequency, mainly because the BESS can start feeding power to the network very quickly while the DG2 is ramping up. When the DG2 power rises high enough, the BESS starts charging, because its SOC setpoint is 80%. The BESS is able to participate in the PDS frequency control while charging by changing its charging power.

V. CONCLUSION

The power system control performance of an offshore supply vessel (OSV) was investigated using model-based simulation and real dynamic positioning (DP) load power data from an actual vessel. The effect of a battery energy storage system (BESS) on the dynamic performance was also analyzed.

Isochronous control was used for the gensets. Isochronous control and average load power estimation were investigated as methods for the power sharing control of a BESS. The parameter sensitivity of the isochronous control with and without a BESS was studied using average load power estimation and isochronous control to form a power reference for the BESS.

Simulation results obtained without a BESS showed that although one genset is enough to produce the power required for the DP operation, the dynamic response of the genset is not fast enough to respond to load changes. Consequently, the vessel has to run two gensets, each on a smaller load to be able to keep its position.

A BESS was added to the vessel to change the dynamic response of the vessel power output. If the vessel is already equipped with the isochronous genset control, the BESS can be controlled using either the average load power estimation or the isochronous control. In the simulations, the average load power estimation produced a slightly higher variance

in the AC network frequency than when using isochronous control. However, under the average load power estimation control, the BESS was able to compensate load fluctuations with smaller AC frequency changes than when operating under the isochronous control.

Two fault cases were also studied. A BESS fault while the vessel is in DP operation was first simulated. As a response to the malfunction, the vessel had to start another genset and modify the isochronous control parameters to move into two-genset isochronous control with equal load sharing. The second fault case was a genset fault during DP operation. As a result of the malfunction, the vessel had to rely on battery power for the short period of time required to start and ramp up the second genset. In this case, it was assumed that the spare genset was already running on a zero power reference and synchronized to the network.

In the BESS fault simulation, the AC frequency dropped to 95% of the nominal frequency for a short period of time. It should, however, be noted that no load shedding was implemented in the simulation, which would be possible on an actual vessel to prevent a blackout. After the BESS malfunction, the second genset was started and the DP operation continued. The change in the system dynamics could be observed from the AC frequency as it fluctuated more without the BESS.

In the genset fault simulation, the fault caused a less than 0.03 p.u. drop in the AC frequency. The system was powered by the BESS while the second genset ramped up. The AC frequency remained within 0.95 p.u. to 1.05 p.u. In this simulation either, load shedding was not implemented.

Based on the results of this study, it can be concluded that all the investigated methods can be used for the BESS power control. The average power estimation method is good for peak shaving, because it reacts immediately to any change in the total load power. Isochronous control might be the easiest method to implement on a vessel already using isochronous control for gensets. While using isochronous control for the BESS, the State-of-Charge (SOC) of the battery must be managed by the power management system (PMS) by modifying the power reference for the BESS. Even when charging, the BESS can take part in the frequency control by changing its charging power. The start–stop method is a modification of isochronous control for the BESS. The start–stop method is able to start and stop gensets according to the load power and modify the isochronous control parameters according to the current configuration. The start–stop method is using the BESS to compensate load fluctuations in the power distribution system (PDS), and it is able to modify the BESS power reference to charge the battery when needed.

REFERENCES

[1] O. Mo and G. Guidi, "Design of minimum fuel consumption energy management strategy for hybrid marine vessels with multiple diesel engine generators and energy storage," in *Proc. ITEC*, Jun. 2018, pp. 537–544.

[2] V. Shagar, S. Jayasinghe, and H. Enshaei, "Effect of load changes on hybrid shipboard power systems and energy storage as a potential solution: A review," *Inventions*, vol. 2, no. 3, p. 21, Aug. 2017, doi: 10.3390/inventions2030021.

[3] T. I. Bø, A. R. Dahl, T. A. Johansen, E. Mathiesen, M. R. Miyazaki, E. Pedersen, R. Skjetne, A. J. Sørensen, L. Thorat, and K. K. Yum, "Marine vessel and power plant system simulator," *IEEE Access*, vol. 3, pp. 2065–2079, 2015, doi: 10.1109/ACCESS.2015.2496122.

[4] A. Lana, A. Pinomaa, P. Peltoniemi, J. Lahtinen, T. Lindh, J.-H. Montonen, K. Tikkanen, and O. P. Pyrhonen, "Methodology of power distribution system design for hybrid short sea shipping," *IEEE Trans. Ind. Electron.*, vol. 66, no. 12, pp. 9591–9600, Dec. 2019, doi: 10.1109/TIE.2019.2892665.

[5] T. I. Bø and T. A. Johansen, "Battery power smoothing control in a marine electric power plant using nonlinear model predictive control," *IEEE Trans. Control Syst. Technol.*, vol. 25, no. 4, pp. 1449–1456, Jul. 2017, doi: 10.1109/TCST.2016.2601301.

[6] L. C. Raveendran and R. G. Devika, "Power fluctuation reduction scheme in marine power plants," in *Proc. WiSPNET*, Mar. 2017, pp. 2037–2040, doi: 10.1109/WiSPNET.2017.8300119.

[7] J. Hou, J. Sun, and H. F. Hofmann, "Mitigating power fluctuations in electric ship propulsion with hybrid energy storage system: Design and analysis," *IEEE J. Ocean. Eng.*, vol. 43, no. 1, pp. 93–107, Jan. 2017, doi: 10.1109/JOE.2017.2674878.

[8] J. Hou, J. Sun, and H. Hofmann, "Battery/flywheel hybrid energy storage to mitigate load fluctuations in electric ship propulsion systems," in *Proc. ACC*, May 2017, pp. 1296–1301, doi: 10.23919/ACC.2017.7963131.

[9] Z. Jingnan and Z. Ying, "Control strategy of hybrid energy storage system in ship electric propulsion," in *Proc. ICMA*, Aug. 2018, pp. 1026–1030.

[10] Y. Guo, M. M. S. Khan, M. O. Faruque, and K. Sun, "Fuzzy logic based energy storage supervision and control strategy for MVDC power system of all electric ship," in *Proc. PESGM*, Jul. 2016, pp. 1–5.

[11] K. Kwon, D. Park, and M. K. Zadeh, "Load frequency-based power management for shipboard DC hybrid power systems," in *Proc. IEEE 29th Int. Symp. Ind. Electron. (ISIE)*, Jun. 2020, pp. 142–147, doi: 10.1109/ISIE45063.2020.9152418.

[12] A. Veksler, T. A. Johansen, R. Skjetne, and E. Mathiesen, "Thrust allocation with dynamic power consumption modulation for diesel-electric ships," *IEEE Trans. Control Syst. Technol.*, vol. 24, no. 2, pp. 578–593, Mar. 2016.

[13] *Guidelines for Vessels With Dynamic Positioning Systems*, Int. Maritime Org., London, U.K., Jun. 1994.

[14] T. A. Johansen, T. I. Bø, E. Mathiesen, A. Veksler, and A. Sørensen, "Dynamic positioning system as dynamic energy storage on diesel-electric ships," *IEEE Trans. Power Syst.*, vol. 29, no. 6, pp. 3086–3091, Nov. 2014, doi: 10.1109/TPWRS.2014.2317704.

[15] M. R. Miyazaki, A. J. Sørensen, N. Lefebvre, K. K. Yum, and E. Pedersen, "Hybrid modeling of strategic loading of a marine hybrid power plant with experimental validation," *IEEE Access*, vol. 4, pp. 8793–8804, 2016, doi: 10.1109/ACCESS.2016.2629000.

[16] X. Shi, Y. Wei, J. Ning, M. Fu, and D. Zhao, "Optimizing adaptive thrust allocation based on group biasing method for ship dynamic positioning," in *Proc. ICAL*, Aug. 2011, pp. 394–398, doi: 10.1109/ICAL.2011.6024750.

[17] A. Lana, K. Tikkanen, T. Lindh, and J. Partanen, "Control of directly connected energy storage in diesel electric vessel drives," in *Proc. EPE/PEMC*, Sep. 2012, pp. 1–7.

[18] *Governing Fundamentals and Power Management*, Woodward, Fort Collins, CO, USA, 2004.

[19] M. Järvisalo, "Keskitehoestimaattorin lisääminen diesel-sähkoiseen hybridijärjestelmään," M.S. thesis, LUT School Energy Syst. (LES), LUT, Lappeenranta, Finland, 2014.

[20] W. F. Oy. *Wärtsilä 34DF Product Guide*. Accessed: Jun. 1, 2022. [Online]. Available: http://www.wartsila.com/docs/default-source/product-files/engines/df-engine/product-guide-o-e-w34df.pdf

[21] R. Pöllänen, "Converter-flux-based current control of voltage source PWM rectifiers—Analysis and implementation," Ph.D. dissertation, Dept. Elec. Eng., Lappeenranta Univ. Technol., Lappeenranta, Finland, 2003.

[22] J. Ollila, "The space vector control of the PWM-rectifier using U/F references," in *Proc. 7th Eur. Conf. Power Electron. Appl. (EPE)*, Trondheim, Norway, Sep. 1997, pp. 4.245–4.249.

[23] P. Peltoniemi, "Phase voltage control and filtering in a converter-fed single-phase customer-end system of the LVDC distribution network," Ph.D. dissertation, Dept. Elect. Eng., Lappeenranta Univ. Technol., Lappeenranta, Finland, 2010.

[24] DNV GL. (Dec. 2015). *Rules for classification. Part 3: Surface Ships, Chapter 3: Electrical Installations*. [Online]. Available: https://rules.dnvgl.com/docs/pdf/DNVGL/RU-NAVAL/2015-12/DNVGL-RU-NAVAL-Pt3Ch3.pdf

[25] T. I. Bo and T. A. Johansen, "Scenario-based fault-tolerant model predictive control for diesel-electric marine power plant," in *Proc. MTS/IEEE OCEANS*, Bergen, Norway, Jun. 2013, pp. 1–5.
[26] K. Kanimozhi and M. V. Kirthiga, "Stability analysis of islanded microgrids," in *Proc. IEEE Int. Conf. Power Electron., Drives Energy Syst. (PEDES)*, Dec. 2016, pp. 1–6, doi: 10.1109/PEDES.2016.7914420.

JAN-HENRI MONTONEN received the M.Sc. degree in electrical engineering from the Lappeenranta–Lahti University of Technology (LUT), Lappeenranta, Finland, in 2012. He is engaged in teaching and research of control engineering, automation, and digital systems with LUT. His research interests include virtual simulation and intelligent control of electrically driven mechatronic systems.

TUOMO LINDH received the B.Sc. degree in mechatronics from the Mikkeli Institute of Technology, Mikkeli, Finland, in 1989, and the M.Sc. and D.Sc. degrees in technology from the Lappeenranta–Lahti University of Technology (LUT), Lappeenranta, Finland, in 1997 and 2003, respectively. Since 1997, he has been with the LUT, where he is currently an Associate Professor. His research interests include generator and motor drives and system engineering, particularly in the areas of distributed power generation, electric vehicles, and mechatronics.

ANDREY LANA received the M.S.E.E. degree from the ETU (LETI), St. Petersburg, Russia, in 2000, and the M.Sc. and D.Sc. degrees in EE from the Lappeenranta–Lahti University of Technology (LUT), Lappeenranta, Finland, in 2008 and 2014, respectively. Since 2014, he has been working as a Full Researcher at the LUT. His current research interests include power system modeling and simulation, optimization of a hybrid propulsion power systems, and microgrid protection and control.

PASI PELTONIEMI (Member, IEEE) received the M.Sc. and D.Sc. degrees in electrical engineering from the Lappeenranta–Lahti University of Technology (LUT), Finland, in 2005 and 2010, respectively. From 2010 to 2014, he was a Postdoctoral Researcher at the Laboratory of Control Engineering and Digital Systems, LUT, where he was an Associate Professor, from 2015 to 2019. He became an Associate Professor of power electronics at the Laboratory of Electrical Drives, LUT, in 2019. His research interest includes modeling and control of power electronic applications, such as dc microgrids, renewable generation, power-to-gas, grid-connected converters, and electric drives.

ANTTI PINOMAA received the M.Sc. and D.Sc. degrees in electrical engineering from the Lappeenranta–Lahti University of Technology (LUT), Lappeenranta, Finland, in 2009 and 2013, respectively. His main research interests include information and communication technologies (ICT) in energy systems, smart grids, microgrid technologies, off-grid systems, and application of the 4G LTE wireless IoT systems integrated with renewable energy sources, and those applications and system platforms covering fields from smart villages to smart cities.

KYÖSTI TIKKANEN received the M.Sc. degree in electrical engineering from the Lappeenranta–Lahti University of Technology (LUT), Lappeenranta, Finland, in 2012. Since 2012, he has been working as a Project Engineer with the Laboratory of Department of Electrical Engineering, LUT. His responsibilities include designing and testing of emulation and measurement setups. His research interests include control and system engineering, and energy efficiency measurements.

OLLI PYRHÖNEN (Member, IEEE) received the M.Sc. and D.Sc. degrees in electrical engineering from the Lappeenranta–Lahti University of Technology (LUT), Finland, in 1990 and 1998, respectively. He has gained industrial experience as a Research and Development Engineer at ABB Helsinki, from 1990 to 1993, and as a CTO of The Switch, from 2007 to 2010. Since 2000, he has been a Professor of applied control engineering at the LUT. In 2010, he received further teaching and research responsibility in the wind power technology at the LUT. His main research interests include modeling and control of electrical drives and other energy conversion systems.